Stem Cell Reports, Volume *5*

Supplemental Information

Reprogrammed Functional Brown Adipocytes Ameliorate Insulin Resistance and Dyslipidemia in Diet-Induced Obesity and Type 2 Diabetes

Tsunao Kishida, Akika Ejima, Kenta Yamamoto, Seiji Tanaka, Toshiro Yamamoto, and Osam Mazda

Species	Gene	ABI Cat. Number
Mouse	*β-Actin*	Mm00607939_s1
Mouse	*Cidea*	Mm00432554_m1
Mouse	*Dio2*	Mm00515664_m1
Mouse	*Klf4*	Mm00516104_m1
Mouse	*Nanog*	Mm02019550_s1
Mouse	*Oct3/4*	Mm03053917_g1
Mouse	*Pgc-1*	Mm01208835_m1
Mouse	*Prdm16*	Mm00712556_m1
Mouse	*Sox2*	Mm03053810_s1
Mouse	*Ucp1*	Mm01244861-m1
Human	*β-ACTIN*	Hs01060665_g1
Human	*ADIPOQ*	Hs00605917_m1
Human	*C/EBP-β*	Hs00270923_s1
Human	*CIDEA*	Hs00154455_m1
Human	*C-MYC*	Hs00153408_m1
Human	*DIO2*	Hs00988260_m1
Human	*LEPR*	Hs00174497_m1
Human	*MT-ND1*	Hs02596873_s1
Human	*PGC-1*	Hs01016719_m1
Human	*PRDM16*	Hs00922674_m1
Human	*UCP1*	Hs00222453_m1

Species	Gene	Primer/probe	Sequence
Human	Exogenous *C/EBP-β*	Forward primer	5'-TTAAGGATCCCAGTGTGGTGGTA-3'
		Reverse primer	5'-AAGTTGGCCACTTCCATGGA-3'
		Probe	5'-CTGGGACCCAGCATG-3'
Human	Exogenous *C-MYC*	Forward primer	5'-AAGCAGGCTCCGCGG-3'
		Reverse primer	5'-AAGTTGGCCACTTCCATGGA-3'
		Probe	5'-CCTCAACGTTAGCTTCA-3'

Supplementary Table S1 (Related to Figures 1, 3, 5, S1, S2, S4, S5, and S6).
Primers and primers for real time-RT-PCR are shown.

Gene	Primers	
PPARγ	S	5'-ATGTAAGTGGATATTGAATAGTTTTTGTTTTG-3'
	AS	5'-CCCATAAATCAAAACATCAATTTCC-3'
UCP1	S	5'-GGAGAGGAAAGGGAAGTAGAGAA-3'
	AS	5'-CCCTCCCATTCCCATTCTCGCTCG-3'

Supplementary Table S2 (Related to Figure 4). PCR primers for bisulfite sequencing are shown. See also Figure 4.

sh*Ucp1* 280	Sense	5'-GATCCGATCTTCTCAGCCGGAGTTTCCTCGAGGAAACTCCGGCTGAGAAGATCTTTTTG-3'
	Antisense	5'-AATTCAAAAAGATCTTCTCAGCCGGAGTTTCCTCGAGGAAACTCCGGCTGAGAAGATCG-3'

sh*Ucp1* 666	Sense	5'-GATCCGCCATCTGCATGGGATCAAACCTCGAGGTTTGATCCCATGCAGATGGCTTTTTG-3'
	Antisense	5'-AATTCAAAAAGCCATCTGCATGGGATCAAACCTCGAGGTTTGATCCCATGCAGATGGCG-3'

sh*Ucp1* 1068	Sense	5'-GATCCGGTCCTGGAACGTCATCATGTCTCGAGACATGATGACGTTCCAGGACCTTTTTG-3'
	Antisense	5'-AATTCAAAAAGGTCCTGGAACGTCATCATGTCTCGAGACATGATGACGTTCCAGGACCG-3'

Supplementary Table S3 (Related to Figure 7). Sequences of sh*Ucp1*. See also Figure 7.

Supplementary Figure S1

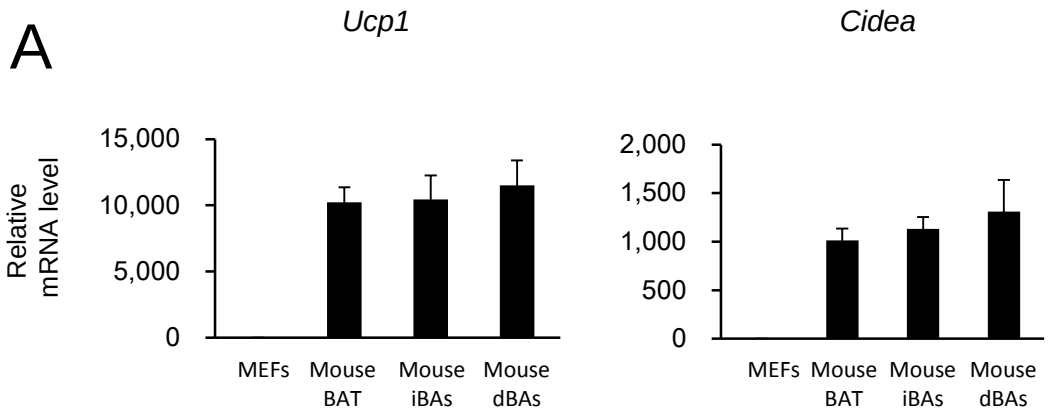

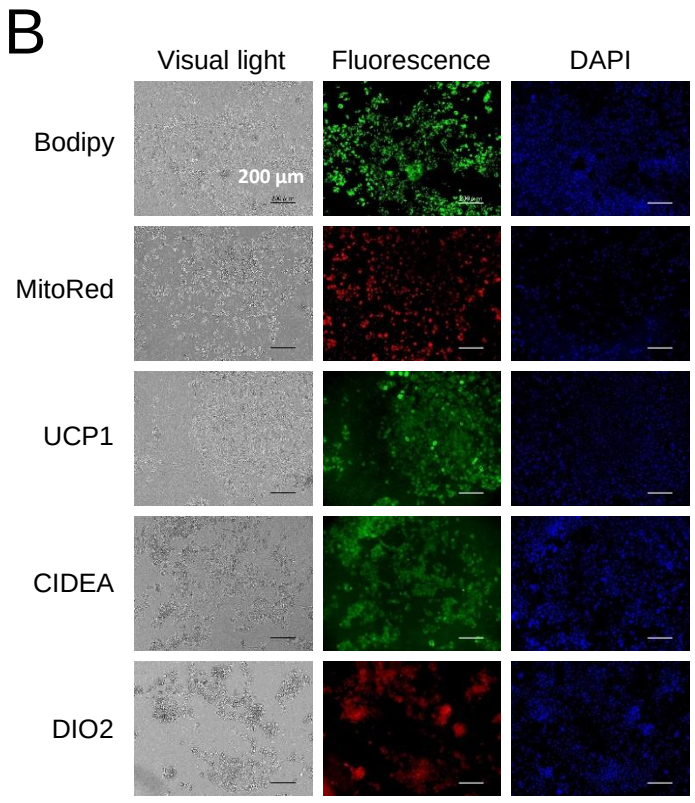

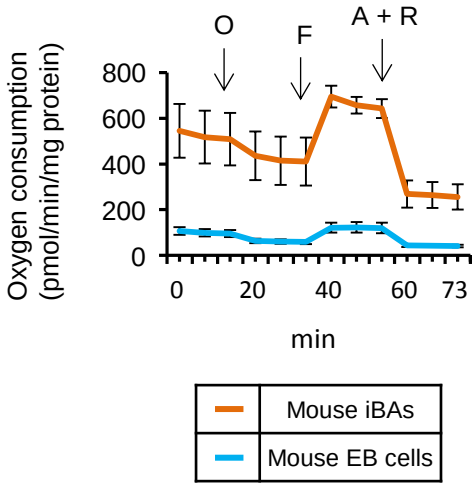

Supplemental Figure S1

Characterization of mouse iBAs (Related to Figure 2). **A**, Mouse iBAs were induced from the iPS cell-derived embryoid body cells by transducing *Prdm16* gene and subsequently culturing for 12 days as described in the Experimental Procedures. Mouse dBAs were induced from MEFs by transducing *PCL* retrovirus vectors and subsequently culturing for 12 days. RNA was extracted from these cells and from the mouse brown adipose tissue (BAT), and real time-RT-PCR analysis was performed using primers/probes specific for *Ucp1* and *Cidea* genes. Values (average ± s.d.) were normalized to *β-Actin* mRNA and expressed relative to values for the MEFs (set to 1.0)(*n*=3 cultures per group). **B**, Mouse iBAs were stained with Bodipy 493/503 (Top) and Mitotracker Red (Second to the top) to visualize lipid droplets and mitochondria, respectively. Other aliquots of cells were incubated with anti-UCP-1, anti-CIDEA and anti-DIO2 antibodies, followed by staining with secondary antibodies. Cell nuclei were also stained with DAPI. Original magnification was x100. **C**, Oxygen consumption of mouse iBAs and embryoid body (EB) cells (average ± s.d.) was evaluated as in Fig. 1E (*n*=3 cultures per group).

Supplementary Figure S2

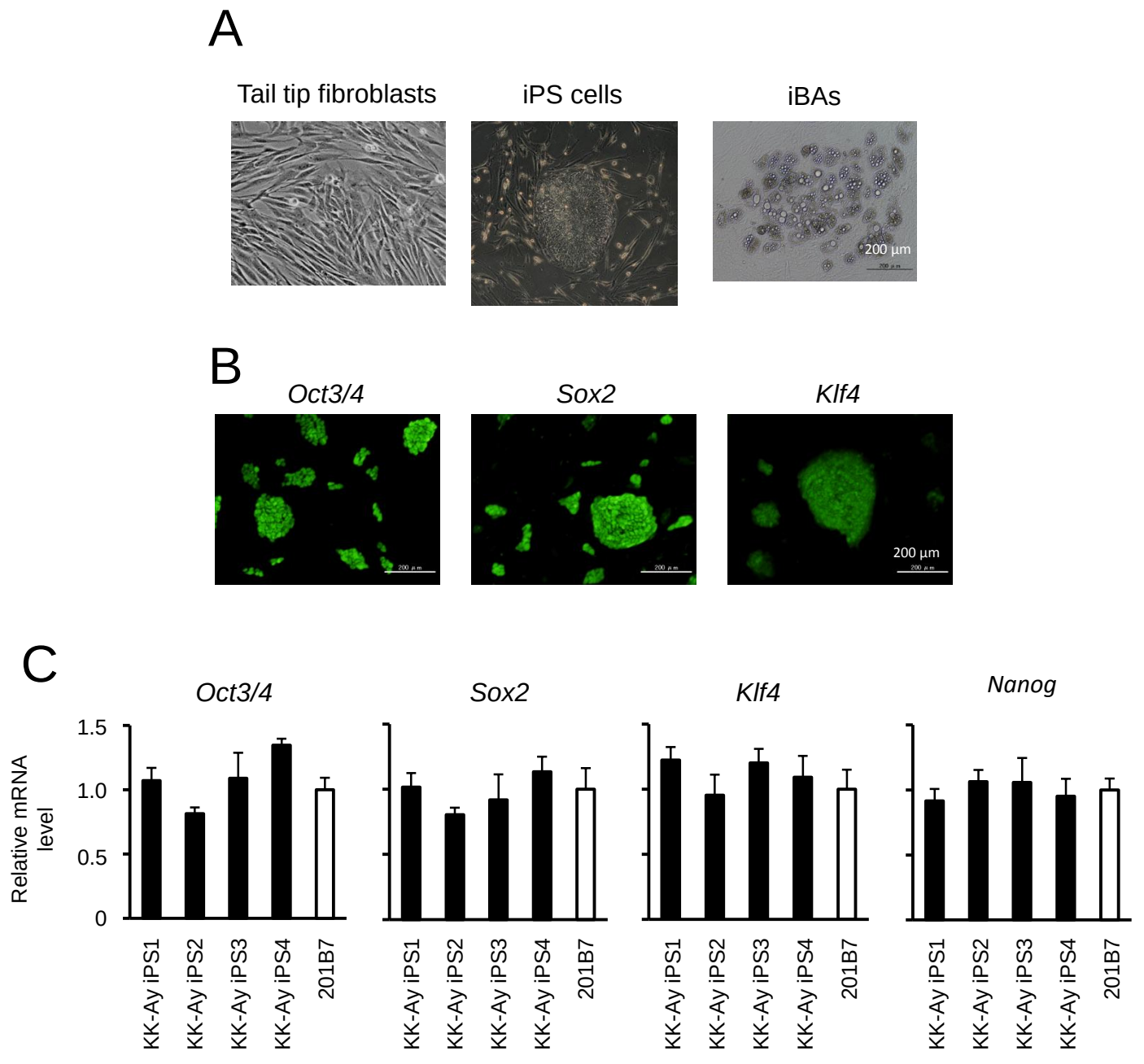

Supplemental Figure S2
iPS cells induced from KK-Ay diabetic mice (Related to Figure 2). Tail tip fibroblasts were obtained from KK-Ay mice, and iPS cells were induced by transducing *Oct3/4*, *Sox2*, *Klf4* and *C-myc* retroviral vectors. iBAs were induced from the iPS cells as described in the Experimental Procedures. **A**, Phase contrast microscopic images of the cells are shown. **B**, KK-Ay iPS cells were immunostained for the indicated transcription factors. **C**, RNA was extracted from four independent iPS cell clones, and mRNA levels for the indicated genes were evaluated by real time RT-PCR. Values (average ± s.d.) were normalized to *β-Actin* mRNA and expressed relative to levels in the 201B7 mouse iPS cells (set to 1.0) (*n*=3 cultures per group).

Supplementary Figure S3

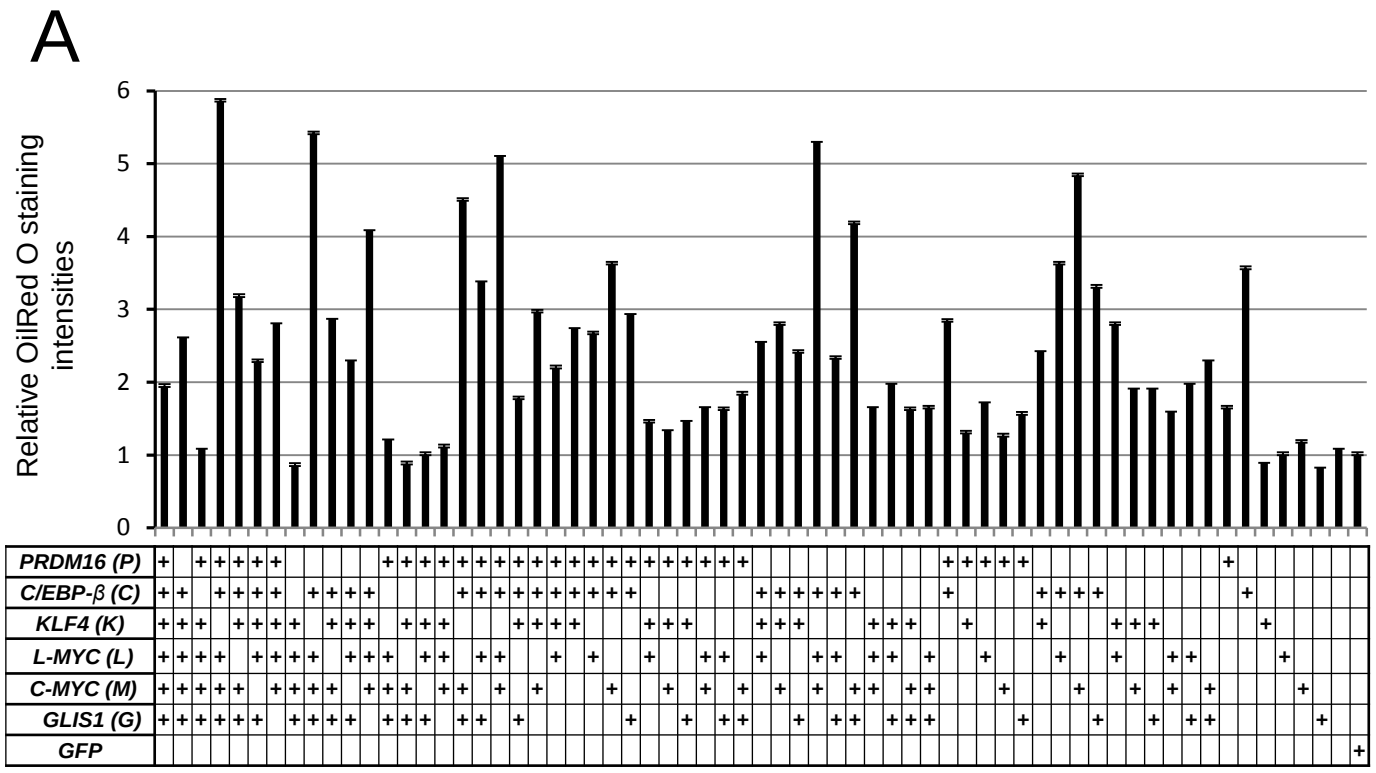

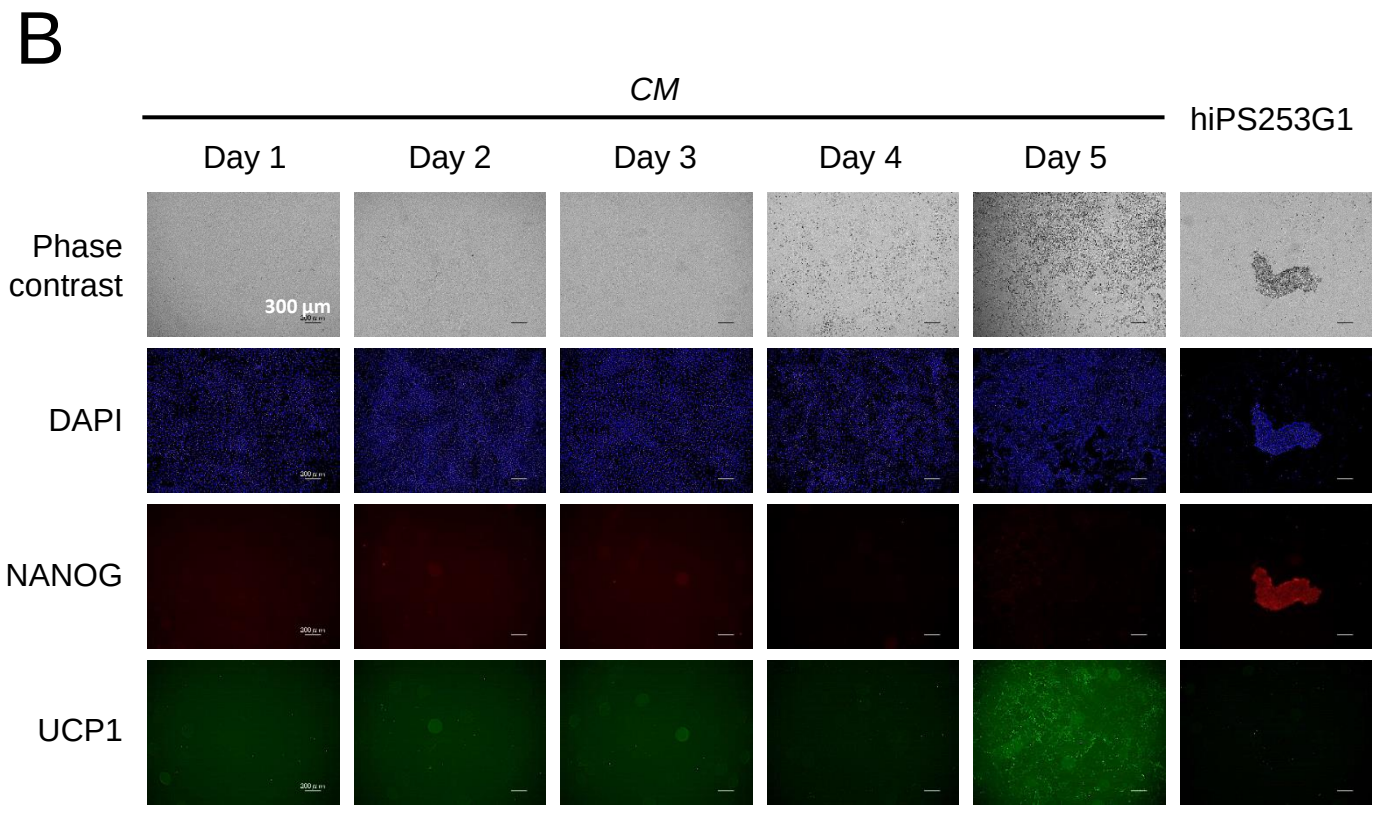

Supplemental Figure S3

Direct conversion of normal human fibroblasts into BAs (Related to Figure 3). **A**, HDFs were seeded into 12-well plate and transduced with mixtures of the indicated genes as described in the Methods ("+" in the Table represents the presence of the corresponding gene). After culturing for 14 days, cells were stained with Oil Red O, and OD_{550} for cell lysates was measured. Values are average ± s.d. (*n*=3 technical replicates). **B**, Human fibroblasts were transduced with *CM* retroviral vectors, and the indicated days later, nuclear staining with DAPI as well as immunostaining with anti-NANOG (cat, RCAB0003P; Repro Cell Inc.) and anti-UCP1 (cat, PAB6905; Abnoba) antibodies were performed. Human iPS cells were also stained as a NANOG-positive control (the rightmost panels). Immunostaining images were obtained using haze reduction. No detectable level of NANOG was demonstrated in fibroblasts between 1 to 5 days after the transduction, while UCP1 was significantly expressed on day 5, indicating that the dBAs were induced from normal fibroblasts without passing a pluripotent stage (*n*=5 cultures per group).

Supplementary Figure S4

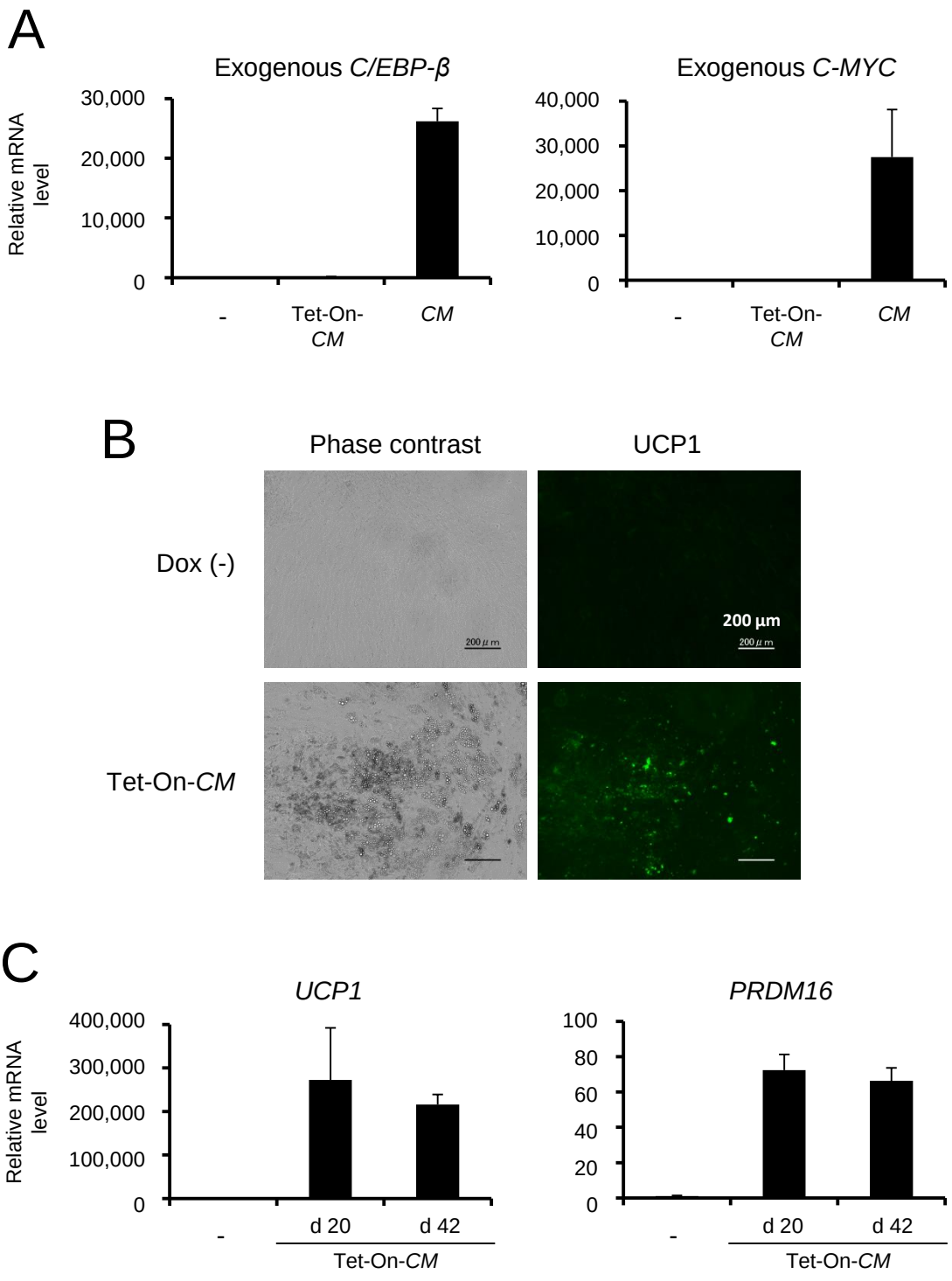

Supplemental Figure S4

Continuous expression of exogenous *C/EBP-β* and *c-Myc* genes may not be essential for dBAs to maintain the BA phenotype (Related to Figure 3). **A**, Human dermal fibroblasts were transduced with retrovirus vectors containing *C* and *M* genes driven by Tet-On promoter (Tet-On-*CM*)(day 0). Cells were cultured as in Figure 3, except that doxycyclin was added to the culture only during the first 20 days. On day 42 colonies with lipid droplets were picked up, and mRNA levels for the retroviral transgenes were evaluated by real time RT-PCR. Non-transduced cells (-) were analyzed as negative control. The cells transduced with conventional *CM* that constitutively expressed *C/EBP-β* and *C-MYC* genes were also analyzed on day 42 as positive control. **B**, Fibroblasts were transduced with Tet-On-*CM* and cultured as in (A). An aliquot of cells were transduced with Tet-On-*CM* and cultured without doxycyclin as control (Dox (-)). On day 42, cells were immuno-stained by anti-UCP1 antibody. Phase contrast and green fluorescence images are shown (magnification, x 100). **C**, Fibroblasts were transduced with Tet-On-*CM* and cultured with doxycycline (days 0-20) and without doxycyclin (days 21-42) as in (A). On days 20 and 42, colonies with lipid droplets were picked up, and mRNA levels for the indicated genes were evaluated. In (A) and (C), values (average ± s.d.) were normalized to *β-ACTIN* mRNA and expressed relative to levels in the non-transduced fibroblasts (set to 1.0) (*n*=3 cultures per group).

Supplementary Figure S5

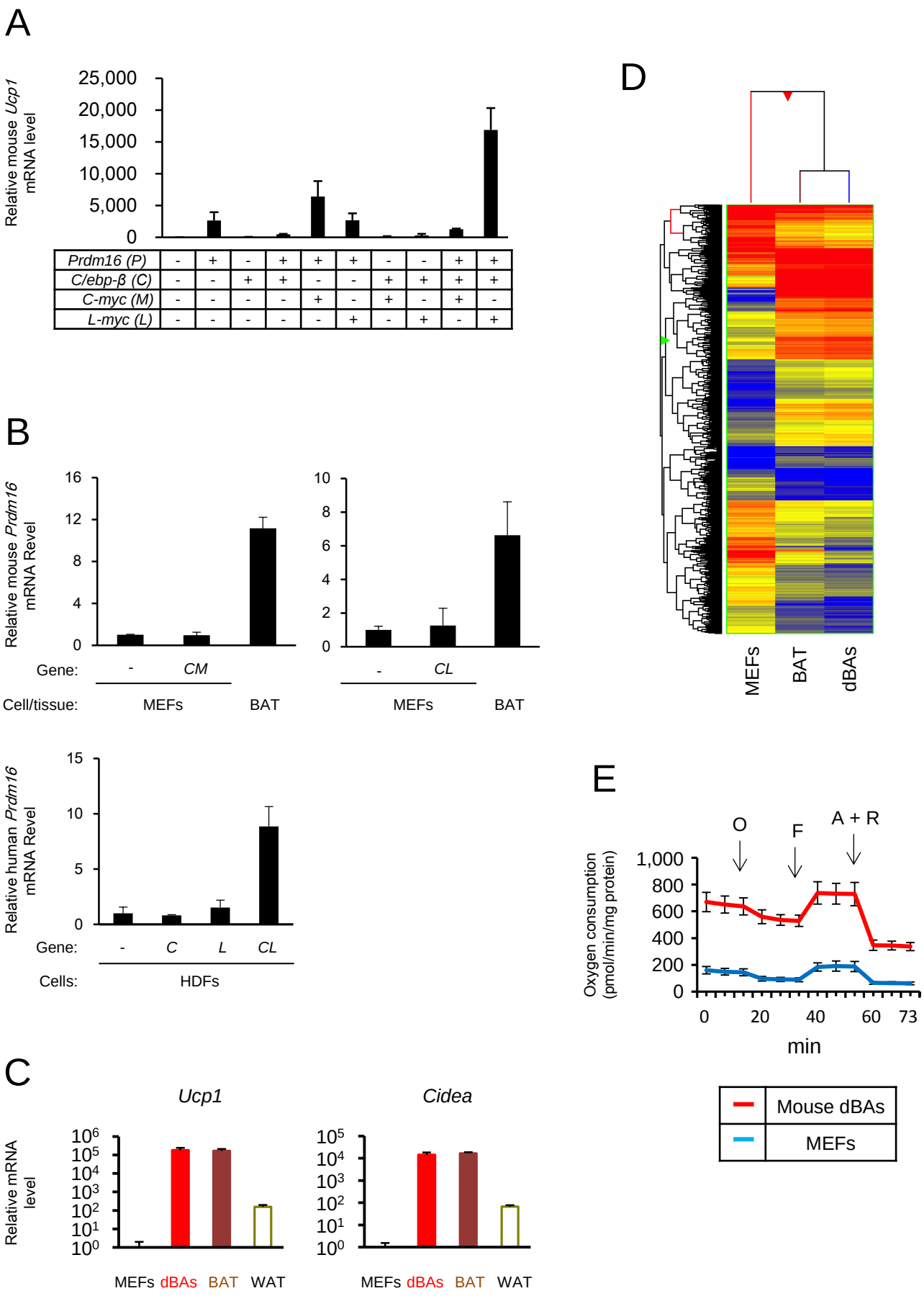

Supplemental Figure S5

Characterization of mouse dBAs (Related to Figure 6). **A**, Mouse fibroblasts were converted into dBAs by transduction with *PCL*. Mouse embryonal fibroblasts (MEFs) were transduced with the indicated retroviral vectors ("+" in the Table represents the presence of the corresponding gene). After culturing for 12 days, *Ucp1* and *β-Actin* mRNA was evaluated by real time RT-PCR. *Ucp1* mRNA levels (average ± s.d.) were normalized to *β-Actin* mRNA and expressed relative to levels in the untransduced MEFs (set to 1.0) (*n*=3 cultures per group). **B**, *Prdm16* mRNA was not induced in mouse fibroblasts by *CM* or *CL* transduction. MEFs (Upper) or HDFs (Lower) were transduced with the indicated retrovirus vectors, and subsequently cultured for 12 days as in (A). RNA was extracted from the cells and real time-RT-PCR was performed to evaluate the mRNA levels of the mouse (Upper) and human (Lower) *PRDM16* genes. As control, RNA extracted from non-transduced fibroblasts and brown adipose tissue (BAT) of mice was also tested. Values (average ± s.d.) were normalized to *β-Actin* mRNA and expressed relative to values for the MEFs (set to 1.0)(*n*=3 cultures per group). The mouse fibroblasts did not significantly express *Prdm16* mRNA after *CM* or *CL* transduction, which was in sharp contrast to human fibroblasts that were provoked to express *PRDM16* mRNA by *CM* or *CL* transduction. This may explain why exogenous *Prdm16* gene is required for direct conversion of mouse fibroblasts into BAs. The transduction of *CL* induced human fibroblasts to express *PRDM16* mRNA at a lower level than *CM* transduction, which may be the reason why *CM* was superior to *CL* in converting human fibroblasts into BAs (Figure S3A). **C**, Mouse dBAs expressed BA markers at high levels. MEFs were transduced with *PCL* retroviral vectors as in (B). After culturing for 12 days, RNA was extracted from the dBAs as well as untransduced MEFs, mouse brown and white adipose tissues (BAT and WAT, respectively). *Ucp1*, *Cidea* and *β-Actin* mRNA was evaluated by real time RT-PCR. Shown are *β-Actin*-normalized *Ucp1* and *Cidea* mRNA levels in each sample (average ± s.d.) relative to those in the untransduced MEFs (set to 1.0) (*n*=3 cultures per group). **D**, Mouse dBAs showed similar gene expression profiles as BAT. MEFs were transduced with *PCL* retroviral vectors as in (B). Twelve days later RNA was extracted from the cells. RNA was also extracted from BAT and untransduced MEFs. DNA microarray analysis demonstrated that among 28,853 genes tested, 4,644 genes were differentially expressed (>2 folds). Heat map and hierarchical clustering analysis of the genes are shown. Red and blue colorations indicate increased and decreased expression, respectively. **E**, Oxygen consumption of the indicated cells (average ± s.d.) was evaluated as in Fig. 1E (*n*=3 cultures per group).

Supplementary Figure S6

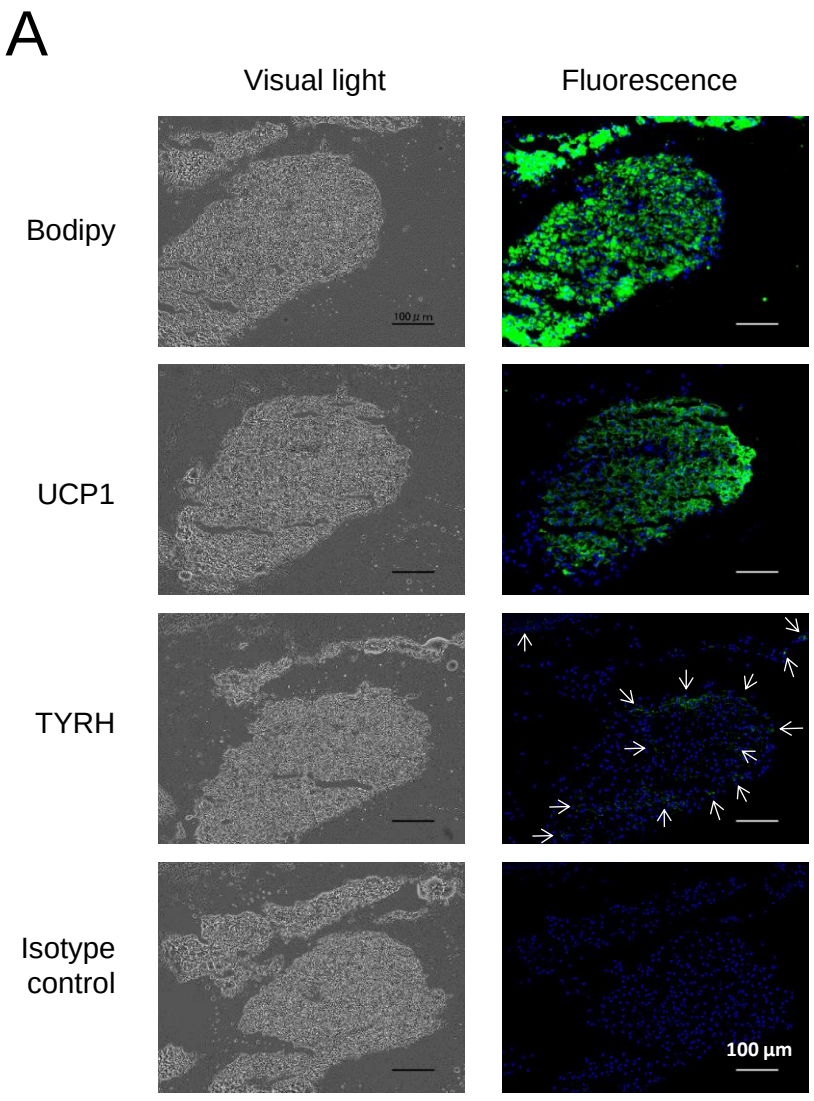

Supplemental Figure S6

Sympathetic innervation in BA graft, and siRNA-mediated silencing of *UCP1* (Related to Figures 6 and 7). **A**, Mouse dBAs were subcutaneously transplanted into syngenic mice as in Figure 6. Twelve days later, mice were sacrificed and graft tissue was excised. Cryosections were stained with Bodipy 493/503 to visualize lipid droplet (Top). Other sections were incubated with anti-UCP1 (R&D Systems, cat no. MAB6158), anti-tyrosine hydroxylase (TYRH)(ImmunoStar, cat no. 22941) and isotype-matched control antibodies, followed by staining with a CF488-conjugated anti-mouse IgG secondary antibody (Biotium, cat no. 20014). The sections were also stained with DAPI to visualize cell nuclei. TYRH-positive cells are indicated by arrows. (Original magnification was x 200). **B**, KK-Ay tail tip fibroblasts were transduced with three different *Ucp1*-specific shRNA via lentiviral vectors. sh*Ucp1* 280, 666 and 1068 sequences (see Supplemental Table S3) were inserted into pGreen puro vector (SBI System Biosciences), and co-transfected into 293TN packaging cells with pCMV-VSV-G, pPACKH1-GAG and pPACKH1-REV plasmids using X-treme Gene 9 transfection reagent (Roche Applied Science). Twenty-four hours later culture medium was replaced by fresh antibiotic-free medium, and after another 24 hours of culturing, supernatant was harvested, filtrated through a 0.45 um pore size filter and used for infection. Five days later, *Ucp1* and *β-Actin* mRNA levels were evaluated by real time-RT-PCR. *Ucp1* mRNA levels (average ± s.d.) were normalized to *β-Actin* mRNA and expressed relative to levels of the non-transduced cells (set to 1.0) (n=3 cultures per group). The sh*Ucp1* 1028 reduced *Ucp1* mRNA level by 86%, and were used in the experiments shown in Fig. 7.

Supplementary Figure S7

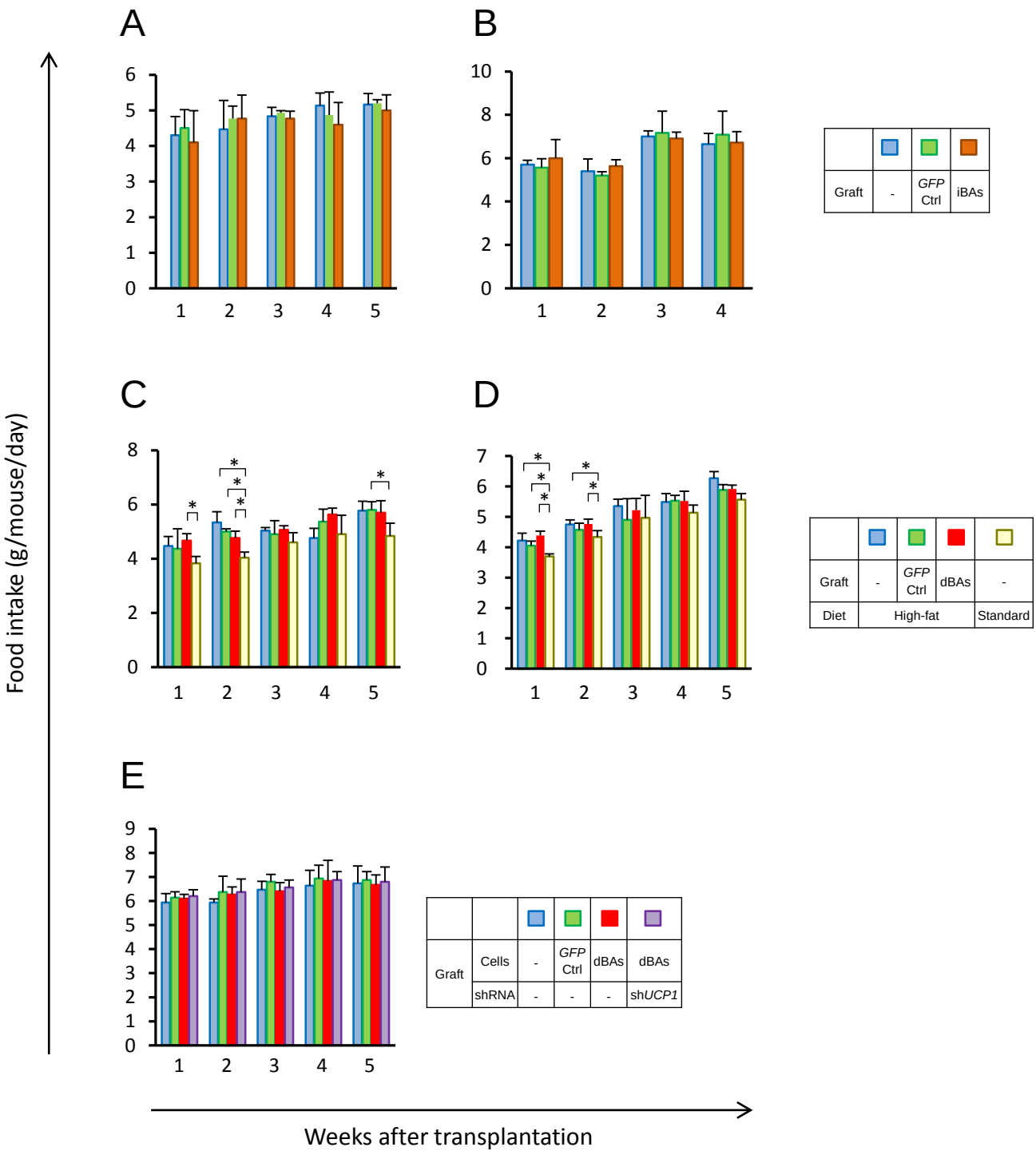

Supplemental Figure S7
Food intake of mice (Related to Experimental Procedures). In the experiments shown in Figs. 2C (A), 2E (B), 6A (C), 6C (D) and 7A (E), food intake of the mice in each group was calculated weekly. Values are average +/- S.D. (*n*=3 (A, B, D and E) and 5 (C) mice per group). In C and D, some mouse groups that were fed the high-fat diet consumed significantly more food than the mice fed a standard chow at some points (*P < 0.05, two-sided Student's t test). But no significant difference was seen among the food consumption of the mouse groups fed high-fat diet, strongly suggesting that the suppression of body weight gain by BA transplantation (Figs. 2C, 2E, 6A, and 7A) was not due to different dietary intake.